OCC-MLLM:Empowering Multimodal Large Language Model For the Understanding of Occluded Objects

Wenmo Qiu
University of Toronto
wenmo.qiu@mail.utoronto.ca

Xinhan Di
Giant Network AI Lab
dixinhan@ztgame.com

Abstract

There is a gap in the understanding of occluded objects in existing large-scale visual language multi-modal models. Current state-of-the-art multimodal models fail to provide satisfactory results in describing occluded objects for visual-language multimodal models through universal visual encoders. Another challenge is the limited number of datasets containing image-text pairs with a large number of occluded objects. Therefore, we introduce a novel multimodal model that applies a newly designed visual encoder to understand occluded objects in RGB images. We also introduce a large-scale visual-language pair dataset for training large-scale visual-language multimodal models and understanding occluded objects. We start our experiments comparing with the state-of-the-art models.

1. Introduction

The latest multimodal dialogue models [1, 3, 5, 7–12, 15, 16], such as MiniGPT-4 [18] and mPLUG-Owl [17] showed that despite significant progress, their description of large-scale language models for occluded objects remains unsatisfactory.

Therefore, we propose OCC-MLLM, a visual language model (shown in Figure 1) designed to understand occluded objects in image conversations. To achieve this goal, we developed a visual encoder module consisting of the common CLIP model [14] and the proposed 3D model [6]. Additionally, a dataset of 600,000 image-text pairs was created and released.

2. Method

First, we formulate the generative process of the proposed MLLM, named Occlusion-Aware Multimodal Large Language Model (OCC-MLLM), for occlusion-aware descriptions of objects at hand. Second, we introduce the formulation details of each proposed OCC-MLLM module.

Third, the proposed occlusion loss is calculated, and an occlusion-aware training strategy for large multi-modal language models is introduced. We represent the generation process of the proposed OCC-MLLM into three parts: input formula, model forwarding, and decoding.

2.1. Formulation of OCC-MLLM Generation

2.1.1 Input Formulation

The input of the proposed OCC-MLLM consists of images and text. Putting aside specific architectural differences, OCC-MLLM generally applies a visual encoder module to extract visual tokens from raw images and uses a cross-modal mapping module to map them to text space as the input of LLM. The mapped visual tokens are used as part of the LLM input along with the text input. The visual tokens are represented as $\mathbf{x}^v = \{x_0, x_1, \ldots, x_{N-1}\}$. N represents the length of the visual token, which is a fixed number in most cases. Similarly, the input text is segmented using a tokenizer and expressed as $\mathbf{x}^p = \{x_N, x_{N+1}, \ldots, x_{M+N-1}\}$. The image and text tokens are then concatenated as the final input $\{x_i\}_{t=0}^{T-1}$ where $T = N + M$.

2.1.2 Model Forward

First, OCC-MLLM is trained in an autoregressive manner using causal attention masks, with each token predicting its next token based on the previous token, formally:

$$\begin{aligned} \mathbf{h} &= \mathrm{F}_{\mathrm{MLLM^{Occ}}}(\mathbf{x}_i) \\ \mathbf{h} &= \{h_0, h_1, \ldots, h_{T-1}\} \end{aligned} \quad (1)$$

where $\mathbf{h}$ represents the output hidden states of the last layer of the $\mathrm{F}_{\mathrm{MLLM^{Occ}}}$.

Second, the hidden state h is projected by applying the vocabulary head $\mathcal{H}$ via $\mathrm{F}_{\mathrm{MLLM^{Occ}}}$. Get the predicted logits (probability) of the next token, and the calculation is as follows:

$$p(x_t \mid x_{<t}) = \mathrm{SoftMax}\left[\mathcal{H}(h_t)\right]_{x_t}, \quad x_t \in \mathcal{X}, \quad (2)$$
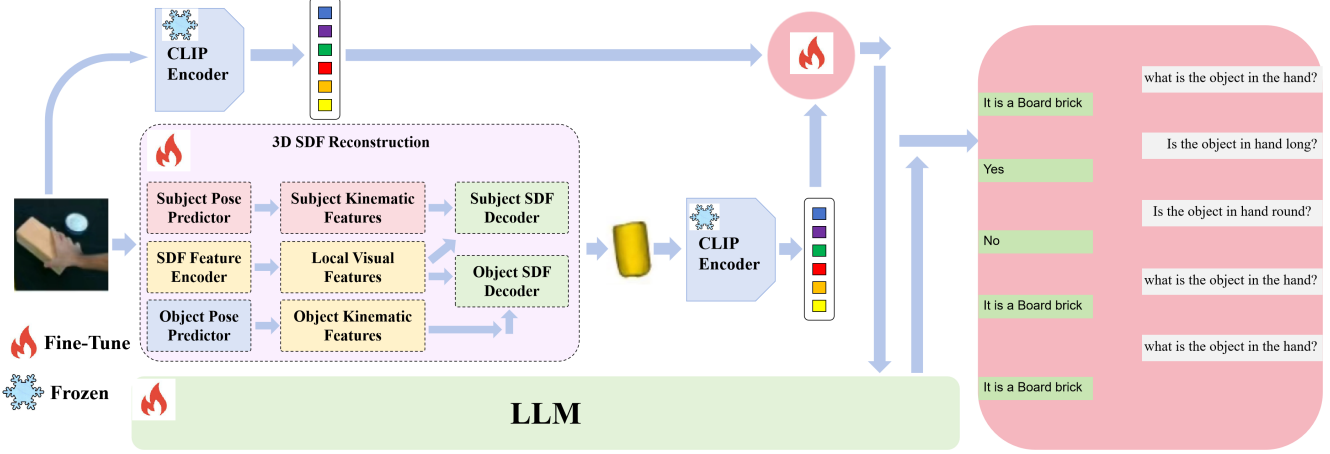
Figure 1. Overview of the Proposed Multi-Modal Vision-Language Model for the Occluded Objects.

where $x_{<t}$ is represented to simplify the sequence $\{x_i\}_{i=0}^{t-1}$ and $\mathcal{X}$ is represents as the whole vocabulary set.

2.1.3 Decoding

After applying logits $p(x_t \mid x_{<t})$, several decoding strategies have been developed, including greedy decoding, Beam Search [2], DoLa, etc. The decoded tokens are concatenated to the last one of the original input text for the next generation round until the end of the generation. The proposed OCC-MLLM applies a beam search strategy [2] is a decoding strategy based on cumulative scores.

2.2. Dual Visual Encoder Module

In forwarding the proposed OCC-MLLM, we designed a new visual encoder module, which consists of two visual encoders. The first visual encoder is the joint CLIP [14], which is used to extract the visual embedding (token) x_v from the RGB input $\mathbf{x}_{v1}$ without a specific occlusion representation. The second visual encoder is used to provide a representation of the occluded object visual embedding(token) $\mathbf{x}_{v2}$. Then, the combined representation is calculated as follows:

$$\mathbf{x}^v = \alpha \cdot \mathbf{x}^{v1} + (1 - \alpha) \cdot \mathbf{x}^{v2} \qquad (3)$$

where $\alpha \in [0, 1]$ represents the transparency level of the visual embedding, $\mathbf{x}^v$ represents the merged embedding.

2.3. Visual Embedding For Occluded Objects

For the second visual encoder to provide the visual embedding (token) $\mathbf{x}_{v2}$ of the occluded object, we designed the second visual encoder f_{3D}, which is composed as follows:

In the first step, a representation of the signed distance function (SDF) [6] of the occluded object in 3D space is calculated (shown in Figure. 2). This representation is merged
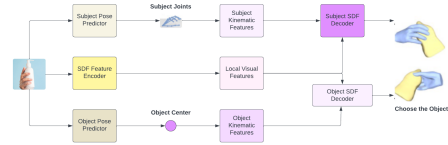

Figure 2. Overview of the proposed second visual encoder reconstruction model f_{3D}. This method reconstructs a mesh of realistic subjects and occluded objects from a single RGB image

into a combination of kinematic and visual features. The SDF of occluded objects and subjects is calculated as follows:

$$\begin{aligned} \text{SDF}_{\text{subject}}(v) &= f_s([e_v; e_h]), \\ \text{SDF}_{\text{object}}(v) &= f_o([e_v; e_o]), \end{aligned} \qquad (4)$$

where f_s and f_o are the subject SDF decoder and the object SDF decoder, respectively, v represents the 3D point.

In the second step, we apply the calculated SDFs of bodies and objects for 3D mesh reconstruction (shown in Figure 2). The computed object $\text{SDF}_{\text{object}}(v)$ already contains the visual representation of the object under occlusion. We reconstruct the 3D mesh M_{obj} of the occluded object and then project it into the 2D RGB space I_{obj}. Then, to make the 2D visual representation I_{obj} easy to use with large language models, we use the visual embedding of $\mathbf{x}_{v2}$ as the extracted embedding of the CLIP model [14]. The above calculation is expressed as follows:

$$\begin{aligned} M_{obj} &= f_{recon}(\text{SDF}_{\text{object}}(v)) \\ I_{obj} &= f_{proj}(M_{obj}) \\ \mathbf{x}_{v2} &= f_{CLIP}(I_{obj}) \end{aligned} \qquad (5)$$
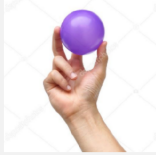
Instruction	Discription
what is the object in the hand?	It's a book
Is the object in hand long?	Yes
Is the object in hand round?	No
Is the object in hand thin?	No
Describe the object in the hand.	It's a long, flat and thick box

Instruction	Discription
what is the object in the hand?	It's a pencil
Is the object in hand long?	Yes
Is the object in hand round?	No
Is the object in hand thin?	Yes
Describe the object in the hand.	It's a long and thin cylinder

Instruction	Discription
what is the object in the hand?	It's a ball
Is the object in hand long?	No
Is the object in hand round?	Yes
Is the object in hand thin?	No
Describe the object in the hand.	It's a roud and small ball

Instruction	Discription
what is the object in the hand?	It's a cup
Is the object in hand long?	Yes
Is the object in hand round?	Yes
Is the object in hand thin?	No
Describe the object in the hand.	It's a long and round cylinder

Instruction	Discription
what is the object in the hand?	It's a hamburger
Is the object in hand long?	No
Is the object in hand round?	Yes
Is the object in hand thin?	No
Describe the object in the hand.	It's a round and thick cylinder

Instruction	Discription
what is the object in the hand?	It's a cellphone
Is the object in hand long?	Yes
Is the object in hand round?	No
Is the object in hand thin?	Yes
Describe the object in the hand.	It's a long, flat and thin box

Instruction	Discription
what is the object in the hand?	It's a bag
Is the object in hand long?	Yes
Is the object in hand round?	No
Is the object in hand thin?	No
Describe the object in the hand.	It's a long, flat and thick box

Instruction	Discription
what is the object in the hand?	lIt's a laptop
Is the object in hand long?	Yes
Is the object in hand round?	No
Is the object in hand thin?	Yes
Describe the object in the hand.	It's a long, flat and thin box

Figure 3. Custom dataset example. The object is occluded. There are five instructions and five corresponding descriptions.

3. Dataset

We collect a large-scale dataset of occluded objects to train the proposed multimodal large language model to understand them.

3.1. Dataset Overview

We released a custom dataset (OCC-HO) containing 600,000 image-text pairs. This dataset was released to describe occluded objects, and to the best of our knowledge, it is for text descriptions of occluded objects. Besides, we manually calculate the occlusions that about a quarter of the objects are occluded on average,

It is important to note that the annotations of each sample are manually checked. Furthermore, we apply the proposed dataset in the instruction tuning stage. All input images are resized to 224×224. (Shown in Figure 3).

3.2. Dataset Annotation

We have provided 5 questions for each image in this dataset. These five questions are: "What's the object in the hand?"; "Is the object in the hand round?"; "Is the object in the hand long?"; "Is the object in the hand thin?"; and "Describe the object in the hand". They are all based on the category, shape, and specific description of the objects in their hands.

Firstly, we used GPT4V [?] to provide preliminary answers to the five questions raised regarding the images. Then, manually check the answers to each image. Man-

ual correction and completion of the answers to the image questions will be done for incorrect or unanswered images. Finally, all the image questions and answers are organized into image pairs to construct a complete dataset of images and texts for occluding objects.

In addition, we also utilized a 3D reconstruction method [6] to reconstruct these occluded objects and obtained 2D images containing only objects, further improving our dataset. In this way, the constructed dataset includes images of occluded objects and two image text datasets that only contain images of unobstructed objects after 3D reconstruction.

4. Experiments and Results

4.1. Experiments on GPT4v[13]

We first test the performance of GPT4v[13] on the testing part of the proposed dataset. Four instructions are applied to test each sample in the testing dataset. And the accuracy is demonstrated in the Table 1. As Table 1 shows, the accuracy of the GPT4v[13] is low. In detail, the accuracy for the instruction 1(What's the object in the hand?) is 0.0361, the accuracy for the instruction 2(Is the object in the hand round?) is 0.6705, the accuracy for the instruction 3(Is the object in the hand long?) is 0.6290, the accuracy for the instruction 4(Is the object in the hand thin?) is 0.5370. It demonstrates that GPT4V[13] cannot achieve satisfactory results for the occluded objects.

4.2. Experiments on MiniGPT4-V2[4])

To effectively evaluate the dataset proposed for occlusion object text description, we fine-tuned two epochs for MiniGPT4-V2[4]. The hyperparameter settings for fine-tuning MiniGPT4-V2[4] are set as the following: The batch size is 16; The learning rate is 0.00002; The weight attenuation coefficient is 0. In addition, to verify the effectiveness of the constructed occluded dataset. As Table 2 shows, in comparison with GPT4V[13], the accuracy is higher for instruction 1, the accuracy is about the same for instruction 2, instruction 3 and instruction 4. The visual encoder of the proposed MiniGPT4-V2[4] is the common clip encoder[14]. (Shown in Figure 1). It demonstrates that fine-tuning on a classical multi-modal large language model[11] with a single joint clip encoder[14] improves the accuracy of the instructions from 0.0361 to 0.3209. However, 0.3209 is still not satisfactory.

4.3. Experiments on the Proposed SDF Encoder[6]

Then, we explore the ability of the SDF encoder[6] for the test description of the occluded objects. At the stage 1, we pretrain the SDF encoder[6] for the task of 3D reconstruction[6] from a single image. At stage 2, we fine-tune the SDF encoder[6], which loads the weights of the reconstruction[6] and then fine-tune the encoder for the task of object classification.

In detail, we use each image of the occluded object in the training dataset and the category of the corresponding object for training. In the testing phase, we calculate the accuracy of the occluded objects given a single image of the occluded object. As Table 2 demonstrates, the accuracy of the instruction 1 is further improved from 0.3209 to 0.5194. We will continue fine-tuning the proposed SDF encoder[6] for the tasks corresponding to the instruction 2-4.

Table 1. Experimental results of GPT4V and MiniGPT4-V2 for the proposed dataset

Model	GPT4v(Zero-shot)	MiniGPT4-V2
Instruction 1	0.0361	0.3209
Instruction 2	0.6705	0.6184
Instruction 3	0.6290	0.5381
Instruction 4	0.5370	0.6017

Table 2. Experimental results of classification of the object category(Instruction 1) for SDF Encoder

Encoder	Task	Accuracy
SDF	Instruction 1	0.5194

4.4. Future Experiments

As the above results demonstrated, the proposed SDF encoder[6] is promising for understanding the occluded objects. We will explore this encoder's ability in subsequent experiments.

Firstly, the SDF encoder[6] continues to be fine-tuned for the task of the instruction 2, instruction 3 and instruction 4. Secondly, the SDF encoder is merged with a classical large language model[11] to provide the text description of the occluded objects. Finally, the SDF encoder[6] and the common clip encoder[14] are merged as the equation 3 shown, and the proposed dual visual encoder module is applied in a classical multi-modal large language model [11] for the description of the occluded objects.

References

[1] Jean-Baptiste Alayrac, Jeff Donahue, Pauline Luc, Antoine Miech, Iain Barr, Yana Hasson, Karel Lenc, Arthur Mensch, Katherine Millican, Malcolm Reynolds, et al. Flamingo: a visual language model for few-shot learning. *Advances in Neural Information Processing Systems*, 35:23716–23736, 2022. 1

[2] Nicolas Boulanger-Lewandowski, Yoshua Bengio, and Pascal Vincent. Audio chord recognition with recurrent neural networks. In *ISMIR*, pages 335–340. Curitiba, 2013. 2

[3] Gongwei Chen, Leyang Shen, Rui Shao, Xiang Deng, and Liqiang Nie. Lion: Empowering multimodal large language model with dual-level visual knowledge. *arXiv preprint arXiv:2311.11860*, 2023. 1

[4] Jun Chen, Deyao Zhu, Xiaoqian Shen, Xiang Li, Zechun Liu, Pengchuan Zhang, Raghuraman Krishnamoorthi, Vikas Chandra, Yunyang Xiong, and Mohamed Elhoseiny. Minigpt-v2: large language model as a unified interface for vision-language multi-task learning. *arXiv preprint arXiv:2310.09478*, 2023. 4

[5] Keqin Chen, Zhao Zhang, Weili Zeng, Richong Zhang, Feng Zhu, and Rui Zhao. Shikra: Unleashing multi-modal llm's referential dialogue magic. *arXiv preprint arXiv:2306.15195*, 2023. 1

[6] Zerui Chen, Shizhe Chen, Cordelia Schmid, and Ivan Laptev. gsdf: Geometry-driven signed distance functions for 3d hand-object reconstruction, 2023. 1, 2, 3, 4

[7] Peng Gao, Jiaming Han, Renrui Zhang, Ziyi Lin, Shijie Geng, Aojun Zhou, Wei Zhang, Pan Lu, Conghui He, Xiangyu Yue, et al. Llama-adapter v2: Parameter-efficient visual instruction model. *arXiv preprint arXiv:2304.15010*, 2023. 1

[8] Tao Gong, Chengqi Lyu, Shilong Zhang, Yudong Wang, Miao Zheng, Qian Zhao, Kuikun Liu, Wenwei Zhang, Ping Luo, and Kai Chen. Multimodal-gpt: A vision and language model for dialogue with humans. *arXiv preprint arXiv:2305.04790*, 2023.

[9] Peng Jin, Jinfa Huang, Fenglin Liu, Xian Wu, Shen Ge, Guoli Song, David Clifton, and Jie Chen. Expectation-maximization contrastive learning for compact video-and-

language representations. *Advances in Neural Information Processing Systems*, 35:30291–30306, 2022.

[10] Junnan Li, Dongxu Li, Silvio Savarese, and Steven Hoi. Blip-2: Bootstrapping language-image pre-training with frozen image encoders and large language models. *arXiv preprint arXiv:2301.12597*, 2023.

[11] Bin Lin, Zhenyu Tang, Yang Ye, Jiaxi Cui, Bin Zhu, Peng Jin, Junwu Zhang, Munan Ning, and Li Yuan. Moe-llava: Mixture of experts for large vision-language models. *arXiv preprint arXiv:2401.15947*, 2024. 4

[12] Haotian Liu, Chunyuan Li, Qingyang Wu, and Yong Jae Lee. Visual instruction tuning. *Advances in neural information processing systems*, 36, 2024. 1

[13] R OpenAI. Gpt-4 technical report. arxiv 2303.08774. *View in Article*, 2:13, 2023. 3, 4

[14] Alec Radford, Jong Wook Kim, Chris Hallacy, Aditya Ramesh, Gabriel Goh, Sandhini Agarwal, Girish Sastry, Amanda Askell, Pamela Mishkin, Jack Clark, Gretchen Krueger, and Ilya Sutskever. Learning transferable visual models from natural language supervision, 2021. 1, 2, 4

[15] Chenfei Wu, Shengming Yin, Weizhen Qi, Xiaodong Wang, Zecheng Tang, and Nan Duan. Visual chatgpt: Talking, drawing and editing with visual foundation models. *arXiv preprint arXiv:2303.04671*, 2023. 1

[16] Zhengyuan Yang, Linjie Li, Jianfeng Wang, Kevin Lin, Ehsan Azarnasab, Faisal Ahmed, Zicheng Liu, Ce Liu, Michael Zeng, and Lijuan Wang. Mm-react: Prompting chatgpt for multimodal reasoning and action. *arXiv preprint arXiv:2303.11381*, 2023. 1

[17] Qinghao Ye, Haiyang Xu, Guohai Xu, Jiabo Ye, Ming Yan, Yiyang Zhou, Junyang Wang, Anwen Hu, Pengcheng Shi, Yaya Shi, et al. mplug-owl: Modularization empowers large language models with multimodality. *arXiv preprint arXiv:2304.14178*, 2023. 1

[18] Deyao Zhu, Jun Chen, Xiaoqian Shen, Xiang Li, and Mohamed Elhoseiny. Minigpt-4: Enhancing vision-language understanding with advanced large language models, 2023. 1